ON THE INFLATION OF A LONG ELASTIC TUBE IN THE PRESENCE OF AXIAL LOAD

STELIOS KYRIAKIDES and YU-CHUNG CHANG

Engineering Mechanics Research Laboratory, Department of Aerospace Engineering and
Engineering Mechanics, The University of Texas at Austin, Austin, TX 78712, U.S.A.

Abstract—When inflating long circular tubes made from some rubber compounds it is possible for
a localization type of instability to occur. The localization takes the form of a bulge which forms
somewhere along the length of the tube. Further inflation results in axial enlargement of the bulged
section. This occurs at a value of pressure which is substantially lower than the pressure at which
the bulge was first initiated. The paper presents experimental and analytical results which show how
the initiation and steady state propagation of such bulges in latex rubber tubes is affected by the
presence of axial tensile load.

NOTATION

A	undeformed tube cross sectional area
F	axial force
H	undeformed tube wall thickness
h	deformed tube wall thickness
l_P	length of bulge profile
P	pressure
P_L	limit pressure
P_I	bulge initiation pressure
P_p	bulge propagation pressure
(R, Θ, Z)	undeformed configuration coordinates
(r, θ, z)	deformed configuration coordinates
R_o, R_i	undeformed tube outside and inside radius
r_o, r_i	deformed tube outside and inside radius
v	internal volume ratio (deformed/undeformed)
$W, \hat{W}$	strain energy density functions
α_n	material constants
λ	circumferential stretch
λ_o	value of λ on outside tube surface
λ_i	value of λ on inside tube surface
λ_z	axial stretch
μ_n	material constants
μ	shear modulus
ω	geometric angle.

INTRODUCTION

The inflation of a long, hollow rubber cylinder is a problem which illustrates quite well the initiation and propagation of an initially localized instability (Chater and Hutchinson, 1984). If the tube is inflated "gradually" the following sequence of events takes place (see also Shield, 1971, 1972; Section 5.3): On application of internal fluid (usually gas) pressure, the tube first expands diametrically in a uniform fashion. At some value of pressure, the deformation localizes to a section a few tube diameters long forming a bulge in the tube. The exact axial position of the bulge depends on imperfections which are typically present as a result of the manufacturing process (e.g. thickness and radius variations, material property variations). At some critical pressure, the bulge experiences a sudden expansion. This usually involves a substantial local increase in diameter. In a tube of finite length, pressurized at a low rate, the sudden increase in volume causes a drop in pressure and a reduction in the diameter of the undisturbed section. As more compressed gas is made available, the bulge grows to a well defined diameter and then stops growing diametrically and starts growing in length. The longitudinal growth of the bulge can take place at a constant level of pressure (propagation pressure—P_p) which is well below the value of pressure at which the bulge was first initiated (initiation pressure—P_I). In addition, during propagation the profile of the propagating front(s) of the bulge retains a constant axisymmetric shape which connects the "small" and "large" diameter sections of the inflated tube.

In the case of a long tube, the growth of the bulge occurs in both directions. The rate at which the bulge grows depends on the rate at which compressed gas is made available to the tube. The bulge propagates until the whole length of the tube has been inflated. Once this is achieved, uniform diametrical expansion of the whole length of the inflated tube resumes.

Chater and Hutchinson (1984) identified most of these characteristics in a simple experiment using a party balloon and established an energy balance type of analysis for predicting the propagation pressure of the bulge. The relative simplicity in both geometry as well as material properties (elastic) makes the problem attractive for analog studies of more complex problems of the same family, such as propagating buckles in long metal tubes under external pressure (Chater and Hutchinson, 1984; Kyriakides and Babcock, 1981; Kyriakides, 1986), propagating necks in some polymeric materials when pulled in tension (Hutchinson and Neale, 1983), and, to some degree, phase transition problems (Abeyaratne and Knowles, 1988).

In this paper the problem is further explored through a combined experimental and analytical effort, with emphasis on establishing the conditions of propagation of bulges in inflated rubber tubes in the presence of axial loading.

EXPERIMENTS

The experiments were conducted on commercially available natural rubber latex tubes. The tubes had nominal outside diameters of 0.5 in (12.7 mm) and wall thickness of 0.063 in (1.60 mm). The test section involved a length of 4–6 ft (1.2–1.8 m). The simple experimental setup used is shown in Fig. 1. One end of the tube was fixed to one outlet of a rigid manifold, and the tube was allowed to hang freely. Axial load was applied by hanging a calibrated weight at the free end of the tube. The lower end of the tube was sealed. The tube was inflated with compressed air. A pressure regulator was used to ensure a constant supply of air. The rate of inflation was controlled manually through a needle-valve downstream of the pressure regulator. The pressure in the system was monitored through a pressure transducer and a pressure gage. During the experiment, the output of the pressure transducer was recorded on an analog strip chart recorder. Changes in the diameter of the tube were measured with calipers. Changes in length were recorded by measuring the distance between markings placed along the length of the undeformed tube.

In preparation for an experiment, the test section of the test specimen was cyclically loaded axially to achieve the required material stability. The tube was then inflated at a slow (quasi static) rate. Figure 2 shows schematically the results of a typical inflation experiment in the presence of no externally applied axial load. The main features of the experiment are as described in the introduction. The bulge gets initiated in a region with the largest material and geometric imperfections. Figure 3 shows a picture of a region experiencing localized deformations which led to localized instability and initiation of a propagating bulge. The picture was taken just before the onset of instability.

The initiation of the bulge occurs in a dynamic fashion. The extent of unloading following the initiation depends on the total volume of air available in the closed system tested (i.e. on the length of the tube and the volume of the manifold and accessories). The steady state axial propagation of the bulge was typically reached when the bulge grew to a length of 3–5 times its diameter. Air was supplied at a rate which resulted in axial expansion of less than one-half bulge diameter per minute. Inflation was continued until the bulge grew to a length of 12–15 diam. Figure 4 presents a sequence of pictures showing the initiation and steady state propagation of a bulge in one of the experiments carried out.

Material properties

The material properties of the latex tubes were measured in separate experiments. Three independent experiments were carried out: (a) Uniaxial experiments on narrow strips cut along the axis and around the circumference of the tube. (b) A pure shear experiment. In this case, a section of the tube was cut along a generator. The cut tube was straightened and clamped between two rigid end plates along the two edges formed by the cut. The

two plates were pulled apart, recording the load and stretch along the direction of pull. The test specimens were made wide enough to ensure that the central portion of the clamped specimen maintained its length in a direction normal to the load. (c) The third experiment was similar to the second, but the test specimen was stretched before clamping. Thus, the central part of the test section had a pre-chosen, constant stretch normal to the direction of the applied load.

The stretches were measured from lines drawn on the undeformed specimens and the loads from calibrated load cells. The results from the three experiments were fitted with the
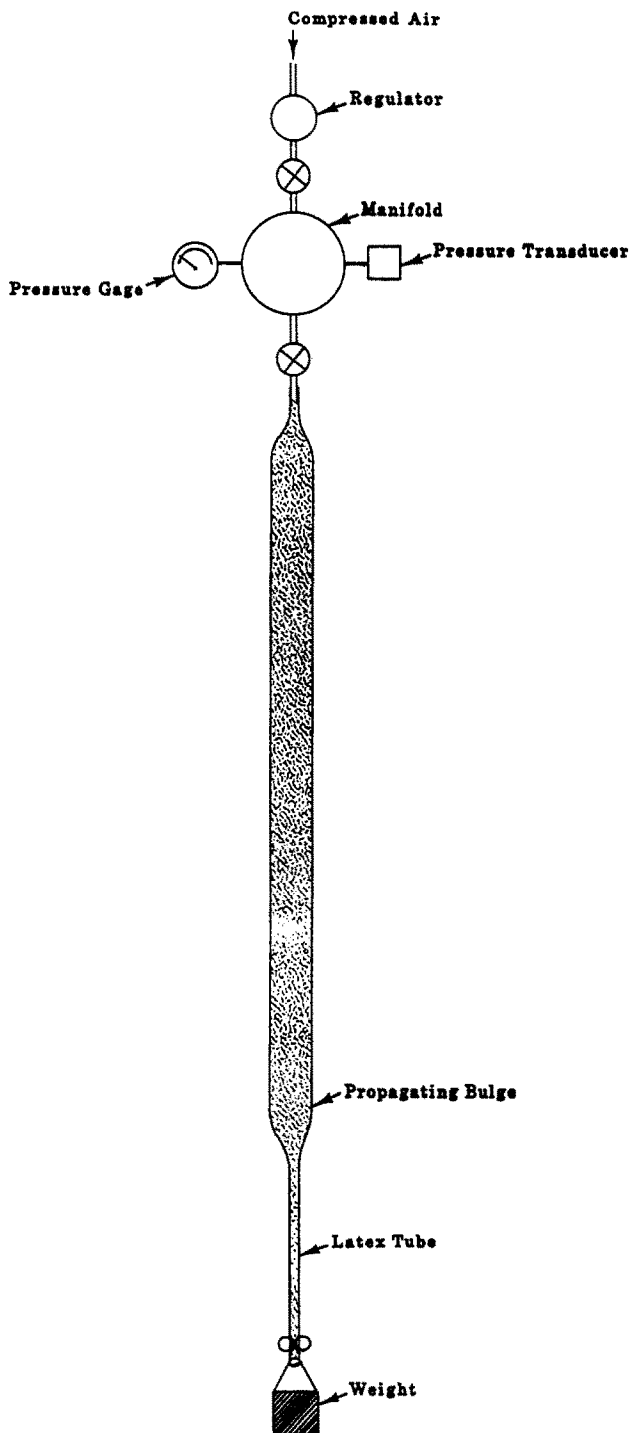
Fig. 1. Experimental set-up.
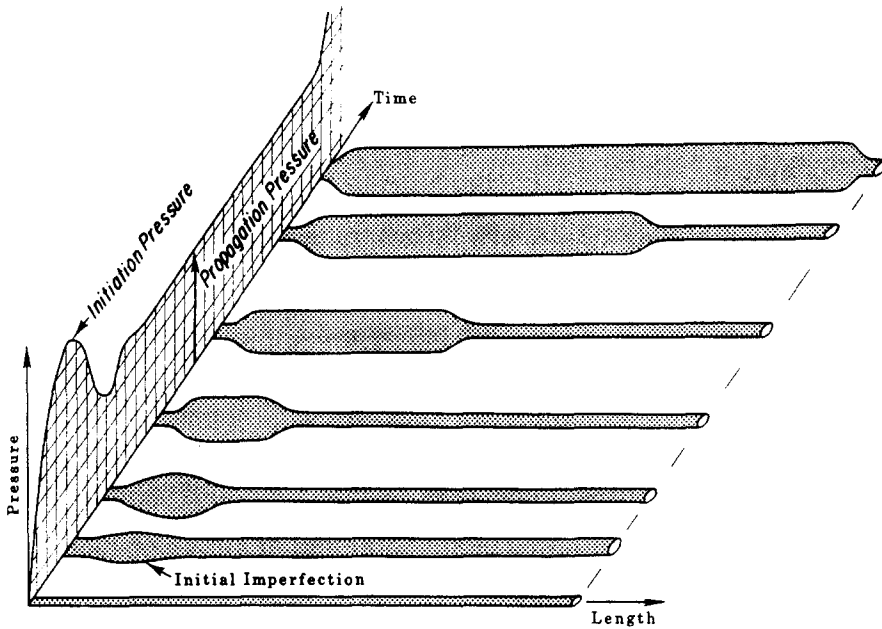
Fig. 2. Schematic representation of a tube inflation experiment.

following strain energy function suggested by Ogden (1972)

$$W = \sum_{n=1}^{3} \mu_n(\lambda_1^{\alpha_n} + \lambda_2^{\alpha_n} + \lambda_3^{\alpha_n} - 3)/\alpha_n \tag{1}$$

where λ_i are the principal stretches and α_n and μ_n are constants found from the experiments. The material was assumed to be incompressible, and the constants were selected so that the three experiments were fitted as well as possible (see Ogden (1972)). In what follows, the following measured values are adopted

$$\mu_1 = 89.4 \text{ psi } (617 \text{ kPa}), \qquad \alpha_1 = 1.30$$
$$\mu_2 = 0.27 \text{ psi } (1.86 \text{ kPa}), \qquad \alpha_2 = 5.08$$
$$\mu_3 = -1.42 \text{ psi } (-9.79 \text{ kPa}), \quad \alpha_3 = -2.00 \tag{2}$$

and

$$\mu = \frac{1}{2} \sum_{n=1}^{3} \mu_n \alpha_n = 60.4 \text{ psi } (416 \text{ kPa}). \tag{3}$$

ANALYSIS

The characteristics of the problem described in the preceding sections can be explained (see Chater and Hutchinson (1984)) by examining the pressure-deformation response of a uniformly inflated (assumed) long elastic tube. An appropriate measure of the deformation is the change in volume (v) in the tube due to changes in length and diameter during the inflation process. For some rubber-like materials the response has the characteristic "s" shape shown in Fig. 5 (see Haughton and Ogden (1979) and Alexander (1971)). The initial tube response (OL) is relatively stiff and is characterized by a limit pressure (P_L). For deformations beyond P_L, the pressure decays to a local minimum (P_M) followed by a brunch (MN) for which the pressure increases with deformation. Thus, in a pressure-

Fig. 3. Localization of deformation of inflated latex tube (picture taken just prior to bulge initiation).
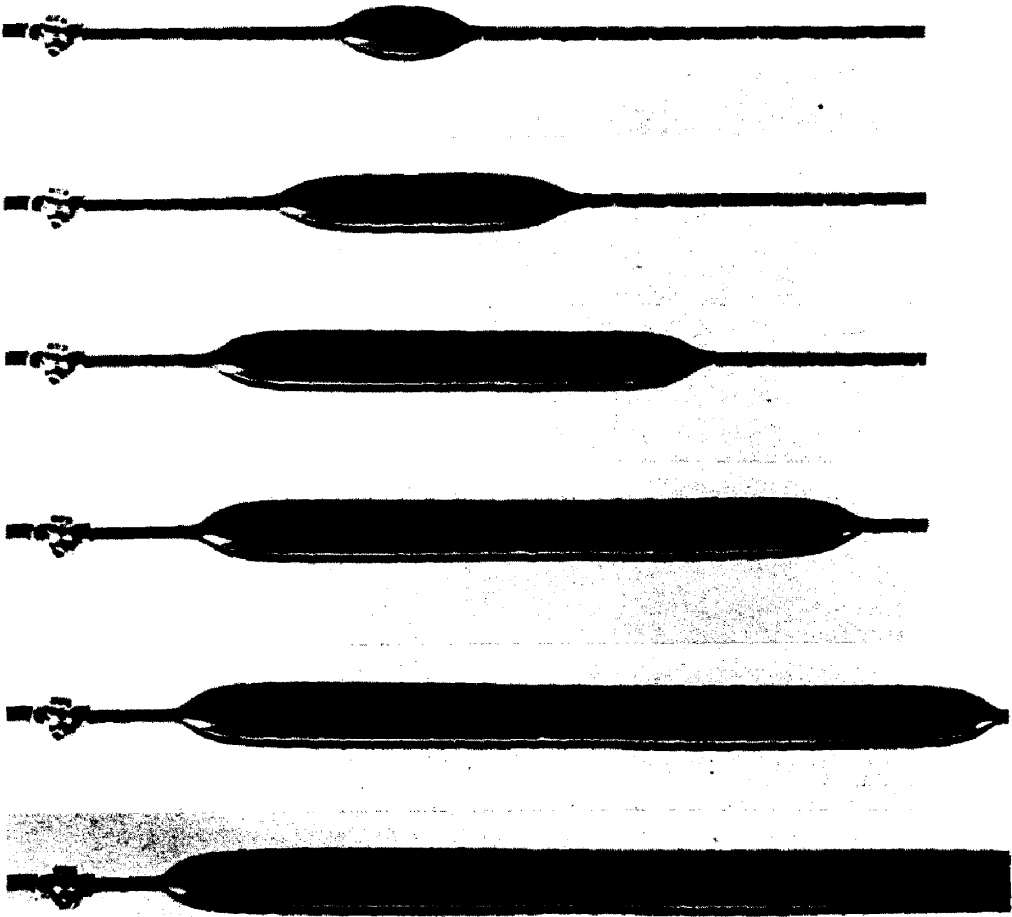

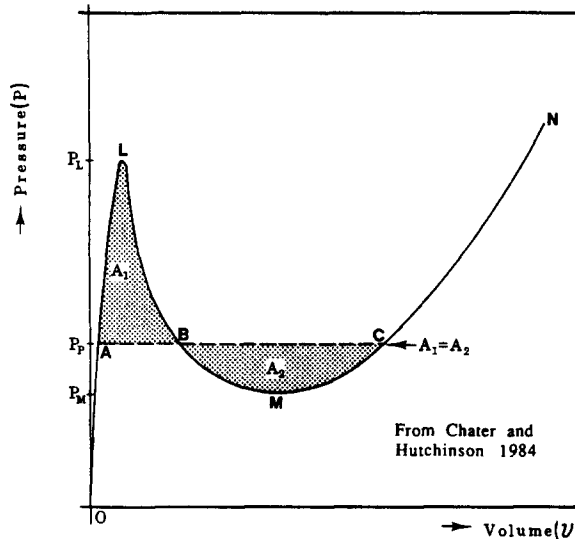Fig. 4. Steady state inflation of a long elastic tube.

Fig. 5. Pressure–volume response of cylindrical inflation of long rubber tube.

controlled experiment, the *LM* part of the response is unstable. During inflation, the tube can be expected to experience a sudden expansion on reaching P_L. Similarly, during deflation (along *NM*) the tube will experience a sudden contraction on reaching P_M.

The scenario outlined above is based on the assumption that the tube deformation is limited to a cylindrical one. In practice, the deformation localizes as discussed in the previous section. Localization occurs at a section along the length which, due to imperfections, has the "lowest" value of P_L. Thus, the initiation pressure recorded in the experiment corresponds to a local limit pressure which is lower than P_L. In an experiment like ours, which involved a fixed finite volume of gas, the pressure in the tube drops following localization. When the initial localized bulge is further inflated, it acquires equilibrium states along *MN*. As the response gets stiffer, it becomes easier for the bulge to grow axially rather than diametrically. As observed experimentally axial expansion can occur under steady state conditions, i.e. the pressure remains constant at the value P_p and the propagation front retains its shape. The propagation front can be viewed as an "imperfection" which progresssively causes the section of tube adjacent to it to jump from equilibrium state *A* to equilibrium state *C* in Fig. 5. In the process, the work done is given by:

$$P_p(v_C - v_A).$$

For an elastic material, the work done during deformation depends only on the initial and final states, i.e. it is independent of the path followed. Thus, if *OLMN* is known, *A* and *C* can be found. As a result, the difference in energy in the tube between states *A* and *C* is given by

$$\int_{v_A}^{v_C} P(v)\, dv.$$

Finally, the propagation pressure can be evaluated by equating the internal and external work done. So

$$P_p = \frac{1}{(v_C - v_A)} \int_{v_A}^{v_C} P(v)\, dv. \tag{4}$$

Expression (4) implies that P_p is at a level which makes areas A_1 and A_2 in Fig. 5 equal (Maxwell line (Chater and Hutchinson, 1984)).

Cylindrical inflation of axially loaded elastic tubes

The finite deformation cylindrical inflation of long, circular, incompressible, elastic tubes has been studied by, among others, Levinson (1962), whereas Haughton and Ogden (1979) and Alexander (1971) considered the effect of axial load in broader studies of the stability of inflated cylinders. Following Haughton and Ogden (1979), we consider a long circular cylinder with undeformed and deformed configurations as defined in Fig. 6 and represented by the cylindrical coordinates (R, Θ, Z) and (r, θ, z), respectively, with

$$R_i \leqslant R \leqslant R_o \quad \text{and} \quad r_i \leqslant r \leqslant r_o.$$

The cylinder is inflated with pressure P and is stretched by an additional axial force F. The material is assumed to be incompressible and the principal stretches are

$$\lambda_r = (\lambda \lambda_z)^{-1}, \quad \lambda_\theta = \frac{r}{R} \equiv \lambda, \; \lambda_z. \tag{5}$$

As a result of incompressibility

$$\lambda_z (r^2 - r_i^2) = (R^2 - R_i^2). \tag{6}$$

In addition, we define

$$\lambda_i = \frac{r_i}{R_i}, \quad \lambda_o = \frac{r_o}{R_o} \quad \text{such that} \quad \lambda_i \geqslant \lambda \geqslant \lambda_o. \tag{7}$$

From (6) and (7)

$$\lambda_i^2 \lambda_z - 1 = \frac{R^2}{R_i^2} (\lambda^2 \lambda_z - 1) = \frac{R_o^2}{R_i^2} (\lambda_o^2 \lambda_z - 1). \tag{8}$$

The material is represented through the strain energy function given in eqn (1). Because of incompressibility, let

$$\hat{W}(\lambda, \lambda_z) = W((\lambda \lambda_z)^{-1}, \lambda, \lambda_z). \tag{9}$$

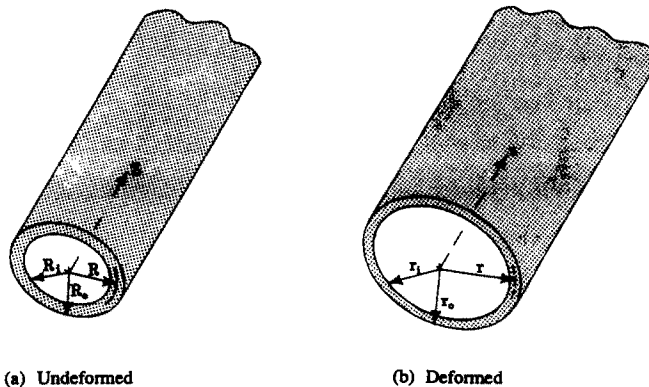By solving the equilibrium equations, the pressure can be related to the deformation

(a) Undeformed   (b) Deformed

Fig. 6. Problem geometry.

as follows:

$$P = \int_{\lambda_o}^{\lambda_i} (\lambda^2 \lambda_z - 1)^{-1} \frac{\partial \hat{W}}{\partial \lambda} \, d\lambda. \tag{10}$$

The net axial force F is given by

$$F = \pi R_i^2 \left\{ (\lambda_i^2 \lambda_z - 1) \int_{\lambda_o}^{\lambda_i} (\lambda^2 \lambda_z - 1)^{-2} \left[2\lambda_z \frac{\partial \hat{W}}{\partial \lambda_z} - \lambda \frac{\partial \hat{W}}{\partial \lambda} \right] \lambda \, d\lambda \right\}. \tag{11}$$

In cases where the tube is "thin", with H and h as the undeformed and deformed wall thicknesses, respectively, i.e. if

$$\frac{R_o - R_i}{R_i} = \frac{H}{R_i} \ll 1 \quad \text{and} \quad R \approx R_o \approx R_i$$

the material incompressibility condition (8) reduces to

$$\lambda_z r h = R H \tag{12}$$

and eqns (10) and (11) reduce to

$$P = \frac{1}{\lambda \lambda_z} \left(\frac{H}{R} \right) \frac{\partial \hat{W}}{\partial \lambda} \tag{13}$$

and

$$F = 2\pi R H \left[\frac{\partial \hat{W}}{\partial \lambda_z} - \frac{1}{2} \lambda \lambda_z^{-1} \frac{\partial \hat{W}}{\partial \lambda} \right] \tag{14}$$

respectively.

The Ogden strain energy function (1) with the measured constants (2) was adopted in eqns (8)–(14) and the pressure–volume response of the inflated tube under fixed applied axial load was calculated numerically. The numerical procedure involved an iterative scheme where, for a fixed value of axial force F and a prescribed value of the circumferential stretch λ_i, the pressure P was evaluated. λ_i was incremented until the complete response was evaluated.

RESULTS

Propagation pressure

Figure 7 shows plots of the pressure–volume responses at different values of axial tension calculated for the latex tube used. The normalizations adopted for the pressure and axial load were guided by the thin walled expressions for P and F in eqns (13) and (14) respectively. A is the undeformed cross-sectional area of the tube and v is the volume acquired in the deformed configuration by a unit volume of the undeformed tube. The response is initially relatively stiff, reaching a limit pressure (P_L) with small change in the volume. The value of P_L decreases with increasing tension. Following the limit pressure, the response drops to a minimum (relative) value of pressure and rises again with a relatively shallow slope. In the process, the tube experiences considerable axial and diametrical expansion. In the presence of axial tension the whole response shifts downwards (lower pressure) but the shape remains approximately the same.

Such responses were used to estimate the value of the bulge propagation pressure at different values of axial tension using the Maxwell construction. The predictions are compared with a set of experimental values in Fig. 8. The predictions are in good agreement with

the measured results. The mean absolute difference is 2.7%, and the maximum difference is 5.6%.

Figure 9 shows a plot of the limit pressure (P_L) calculated as a function of the applied axial tension. P_L is shown to be reduced by tension. We note that P_L represents the critical instability pressure in a pressure controlled "experiment", provided the tube remains
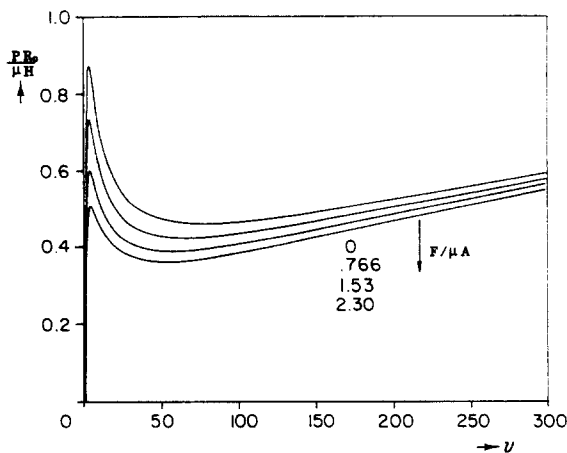

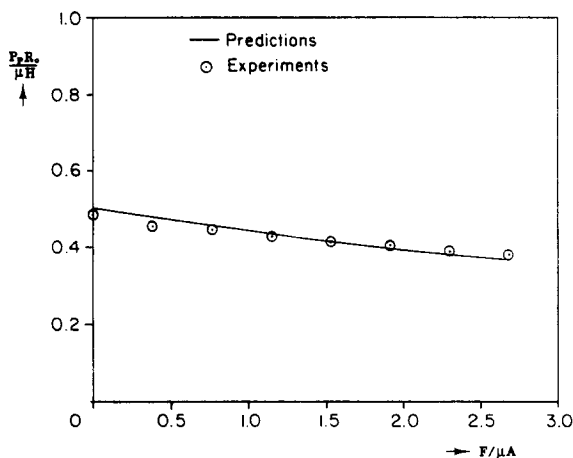Fig. 7. Pressure–volume responses of inflated tube at different values of axial tension.

Fig. 8. Comparison of experimental and predicted values of propagation pressure at different values of axial tension.
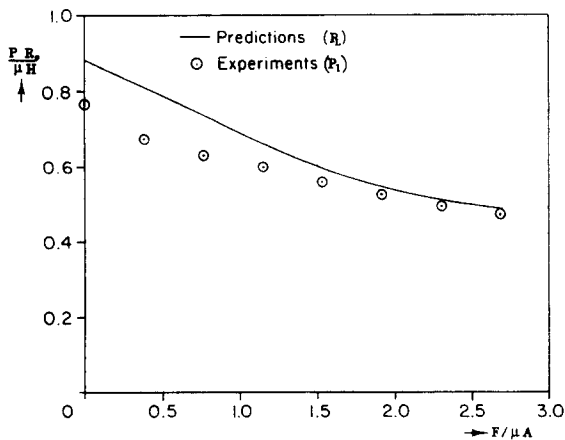
Fig. 9. Comparison between predicted limit pressures and measured bulge initiation pressures at different values of axial tension.

cylindrical. As mentioned earlier, in the course of the experiments carried out, it was observed that inflation caused deformation to localize to a section of tube 10–15 diam. (deformed) long. The localized deformation led to the formation of the localized bulge at the pressure we defined as the initiation pressure, P_I. We also note that the localization process can be influenced by both material as well as geometric imperfections.

The initiation pressures recorded in the experiments which involved different values of axial tension are also presented in Fig. 9. As expected, the initiation pressures are lower than the limit pressures for all values of tension; however, the difference decreases substantially for higher values of tension. One cause of the reduction in the difference between the two pressures may be the reduction in shape imperfections present in the tubes as a result of the applied axial tension.

In the course of the bulge propagation experiments, the diametral and axial changes in the bulged and unbulged sections of the test specimens were measured. Figures 10 and 11 show comparisons between predicted and measured results for the circumferential and axial stretches. The predicted results were extracted from equilibrium states A and C, as shown in the figures. The agreement between the two sets of results is in general good. The biggest discrepancy is observed in the results for the circumferential stretch of the bulged section. The predictions become progressively lower than the measurements with increasing axial tension. The appropriateness of the strain energy function [eqns (1) and (2)] used
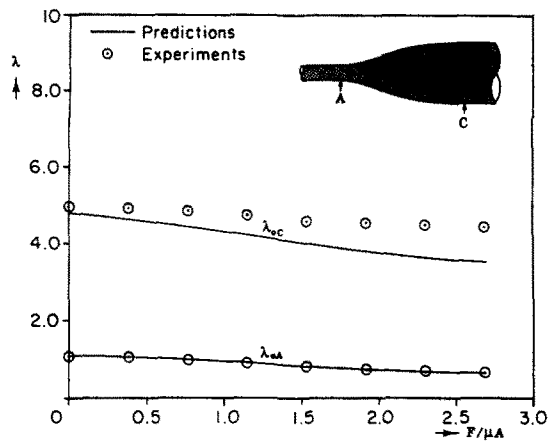

Fig. 10. Comparison between measured and predicted results of circumferential stretches in small and large sections of a propagating bulge.
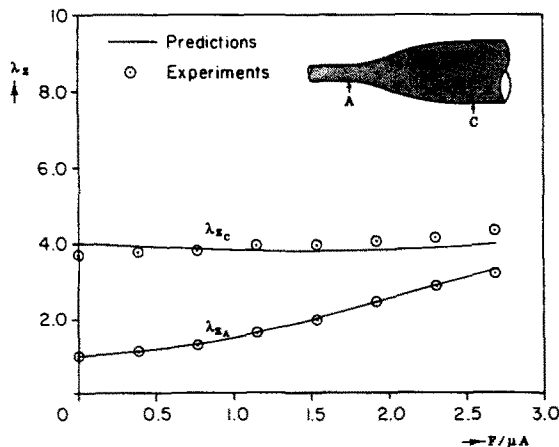

Fig. 11. Comparison between measured and predicted results of axial stretches in small and large diameter sections of a propagating bulge.

could not be tested at very high stretches in the relatively simple biaxial material experiments carried out. Thus, the difference in the results of λ_{oC} can be attributed to the inadequacy of the constitutive representation used at high stretches. This discrepancy seems to have a small effect on the predictions of the propagation pressure.

All results presented above were obtained numerically from the complete analysis of a thick walled elastic tube [eqns (6)–(11)]. Figure 12 shows a comparison between the pressure volume response obtained from the thick walled formulation and that obtained by adopting the thin wall approximation [eqns (12)–(14)]. In view of the relatively low value of R/H of the tube used, some difference in the two predictions is observed in the post-limit pressure part of the response. However, the difference in the predicted propagation pressures is only 0.7%. This order of error was found to be true for all values of axial tension used in the experiments.

Profile of propagation of bulge

The steady state propagation of the bulge involves a transition region (regions) which joins the small and large diameter sections of the bulged tube. We will refer to this transition region as the profile of propagation. Figure 13 shows pictures of three profiles obtained in experiments involving different values of applied tension. The profile shape clearly varies with tension. In this section, we seek to establish the shape and length of the profile.

The analysis required for establishing the geometry of the profile is simplified if the thin wall approximation can be adopted. Encouraged by the reasonably good predictions of the pressure–volume response made through the thin wall approximation (Fig. 12), the tube is approximated as a thin membrane. One of the equations of equilibrium required for axisymmetric deformations of initially circular cylindrical membranes was shown by Pipkin (1968) to reduce to

$$\hat{W} - \lambda_z \frac{\partial \hat{W}}{\partial \lambda_z} = \text{const.} \equiv C_o. \tag{15}$$

The second equation of equilibrium can be obtained by considering equilibrium of forces of a free body diagram involving a cut perpendicular to the tube axis. If the cut is made at a position at which the profile has radius $r(r_A \leqslant r \leqslant r_C)$, then axial equilibrium requires that

$$\pi R^2 \lambda^2 P_p + F = 2\pi R H \frac{\partial \hat{W}}{\partial \lambda_z} \cos \omega \tag{16}$$
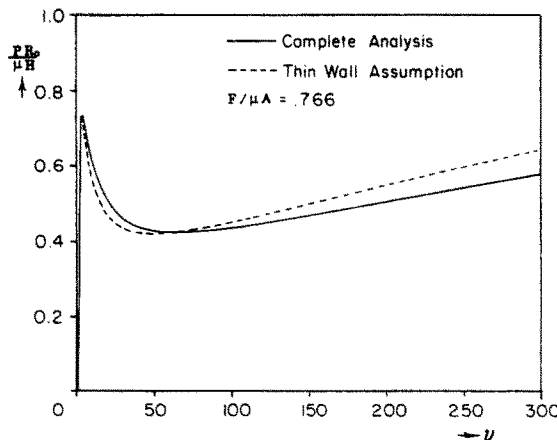

Fig. 12. Pressure–volume responses from complete and approximate analyses.

$\mathbf{F}/\mu\mathbf{A} = 0$

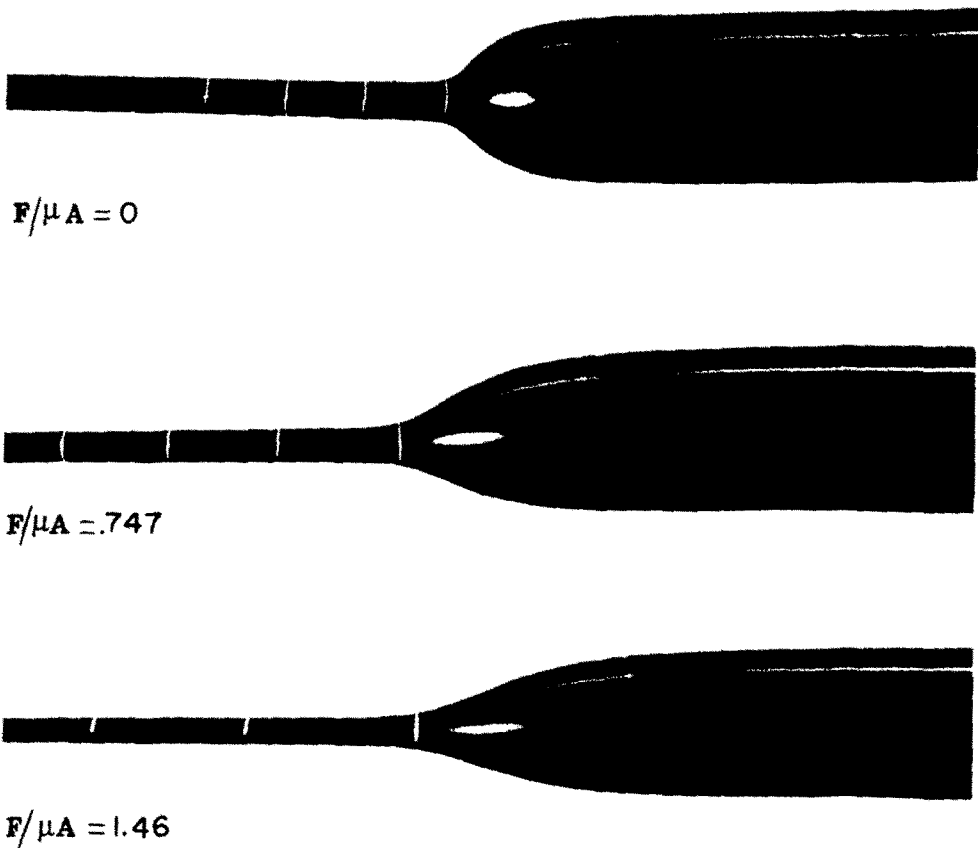$\mathbf{F}/\mu\mathbf{A} = .747$

$\mathbf{F}/\mu\mathbf{A} = 1.46$

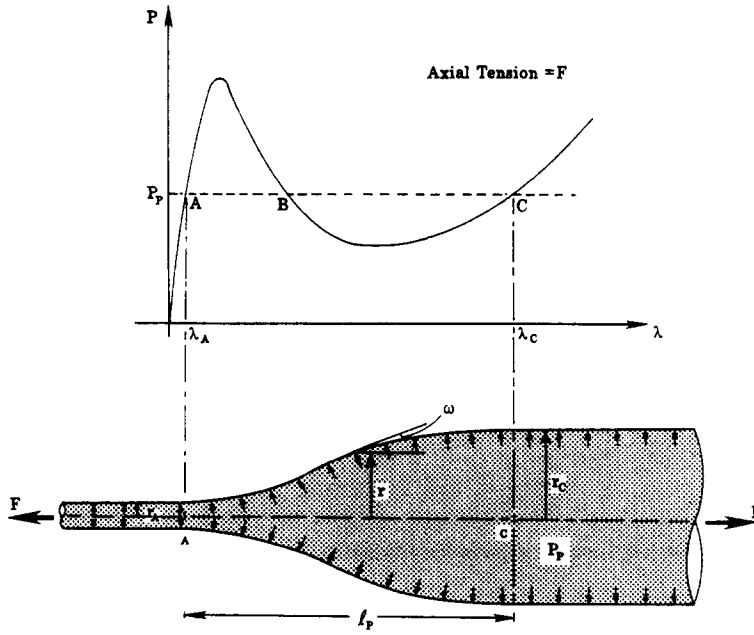Fig. 13. Profiles of propagating bulges at different values of axial tension.

Fig. 14. Geometry of the profile of a propagating bulge and equilibrium states of cylindrical sections.

where ω is defined in Fig. 14 and $\lambda = r/R$. This expression is a simple extension of results obtained by Yin (1977) for the pure pressure case. We identify points A and C as the beginning and end of the profile as shown in Fig. 14. The stretches (λ, λ_z) at these points can be obtained directly from equilibrium states A and C on the $P - \lambda$ response of a long cylindrical tube. This in turn can be obtained from eqns (12)–(14), as described in the previous section. Thus, the constant C_o can be evaluated from either of these equilibrium states. At intermediate points, the solution is obtained as follows: Select a value of $r_A < r < r_C$ (i.e. $\lambda_A < \lambda < \lambda_C$). For a chosen value of λ, find the corresponding λ_z from eqns (12)–(15). The value of ω can then be obtained from (16). Finally, the axial position along the length of the profile can be obtained from

$$\int_o^z \mathrm{d}z = R \int_{\lambda_A}^{\lambda} \frac{\mathrm{d}\lambda}{\tan \omega}. \tag{17}$$

The length of the profile, l_p, is given by

$$l_p = R \int_{\lambda_A}^{\lambda_C} \frac{\mathrm{d}\lambda}{\tan \omega}. \tag{18}$$

Due to the complexity of the strain energy function adopted [eqn (1)], the procedure described was carried out numerically. The singular integral (17) was evaluated using Gaussian quadrature. The number of integration points was varied until the solution was convergent.

Figure 15 shows a set of profiles established numerically for the geometric and material parameters of the tube used in the experiment. In the presence of axial tension, the profile gets elongated in the axial direction and contracts diametrically. Figure 16 shows how the length of the calculated profile, l_p, increases with tension. These predictions are, in general, in agreement with the experimental observations.
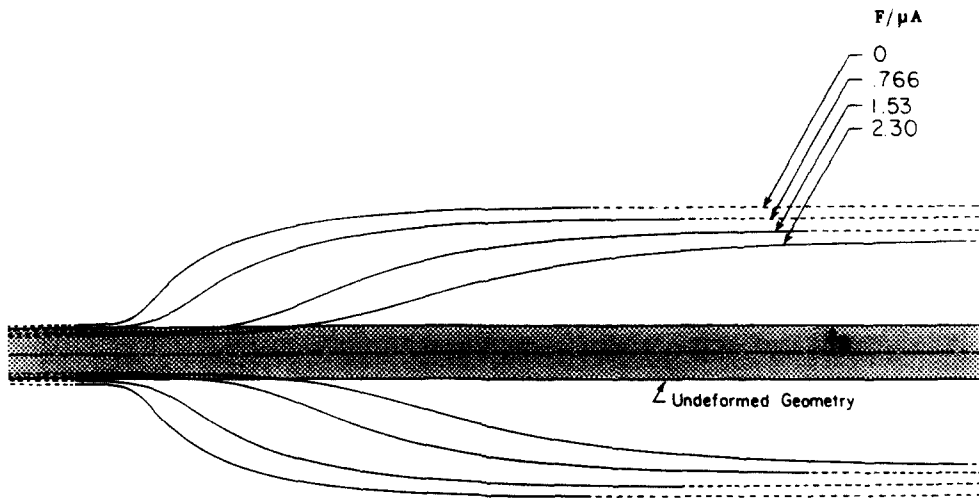
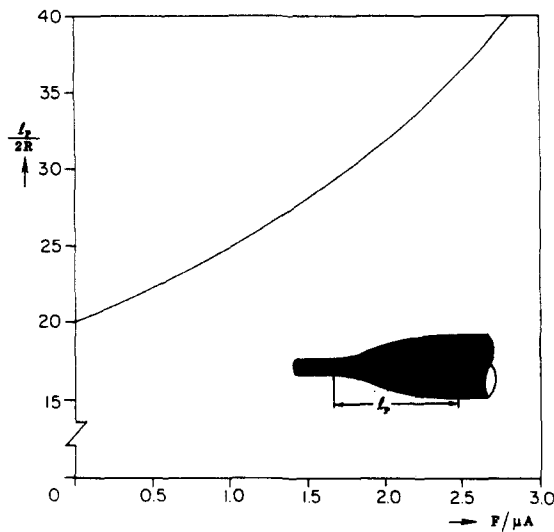Fig. 15. Profiles of propagating bulge for different values of axial tension (predictions).

Fig. 16. Predicted length of profile as a function of axial tension.

CONCLUSIONS

It has been demonstrated that a bulge can be initiated and propagated in a long rubber-like circular tube if the material characteristics are such that the pressure–volume response of cylindrical inflation has the characteristic "s" shape shown in Fig. 5. For such materials the pressure of steady state, quasi static propagation of the bulge is constant. Its value can be calculated directly from the pressure–volume response mentioned above using the Maxwell construction as suggested in Chater and Hutchinson (1984).

The pressure at which the bulge is initiated was shown to be in general lower than the limit pressure of the same response. Thus the localization process which governs this onset of instability is probably influenced by initial geometric and material imperfections.

For the range of axial tension considered it was shown that axial tension lowers both the initiation as well as the propagation pressures of the bulge, results to which every young handler of toy balloons is privy.

The geometry of the profile of propagation of the bulge was shown to be easily extracted from axial equilibrium of the transition region. Both the length as well as the shape of the profile vary substantially with axial tension.

REFERENCES

Abeyaratne, R. and Knowles, J. K. (1988). On the dissipative response due to discontinuous strains in bars of unstable elastic materials. *Int. J. Solids Structures* **24**, 1021–1044.

Alexander, H. (1971). The tensile instability of an inflated cylindrical membrane as affected by an axial load. *Int. J. Mech. Sci.* **13**, 87–95.

Chater, E. and Hutchinson, J. W. (1984). On the propagation of bulges and buckles. *ASME J. Appl. Mech.* **51**, 269–277.

Haughton, D. M. and Ogden, R. W. (1979). Bifurcation of inflated circular cylinders of elastic material under axial loading, Parts I and II. *J. Mech. Phys. Solids* **27**, 179–212 and 489–512.

Hutchinson, J. W. and Neale, K. W. (1983). Neck propagation. *J. Mech. Phys. Solids* **31**, 405–426.

Kyriakides, S. and Babcock, C. D. (1981). Experimental determination of the propagation pressure of circular pipes. *ASME J. Press. Vessel Tech.* **103**, 328–336.

Kyriakides, S. (1986). Propagating buckles in long confined cylindrical shells. *Int. J. Solids Structures* **22**, 1579–1597.

Levinson, M. (1962). The finite strain behavior of incompressible hollow cylinders and spheres under internal pressure. GALCIT Report SM 62-48.

Ogden, R. W. (1972). Large deformation isotropic elasticity—on the correlation of theory and experiment for incompressible rubber-like solids. *Proc. Royal Society London* **A326**, 565–584.

Pipkin, A. C. (1968). Integration of an equation in membrane theory. *J Appl. Math. Phys. (ZAMP)* **19**, 818–819.

Shield, R. T. (1971). On the stability of finitely deformed elastic membranes; Part I: Stability of a uniformly deformed plane membrane. *J. Appl. Math. Phys. (ZAMP)* **22**, 1016–1028.

Shield, R. T. (1972). Part II: Stability of inflated cylindrical and spherical membranes. *J. Appl. Math. Phys. (ZAMP)* **23**, 16–34.

Yin, W.-L. (1977). Non-uniform inflation of a cylindrical elastic membrane and direct determination of the strain energy function. *J. Elasticity* **7**, 265–282.